Partial restoration of chiral symmetry inside hadrons

Takumi Iritani[*a], **Guido Cossu**[b]**, and Shoji Hashimoto**[bc]

[a]*Yukawa Institute for Theoretical Physics (YITP), Kyoto 606-8502, Japan*
[b]*High Energy Accelerator Research Organization (KEK), Ibaraki 305-0801, Japan*
[c]*School of High Energy Accelerator Science, The Graduate University for Advanced Studies
(Sokendai), Ibaraki 305-0801, Japan*
E-mail: `iritani@yukawa.kyoto-u.ac.jp`

By using the overlap-Dirac operator eigenmodes, we investigate spatial distribution of the chiral condensate around static color sources for both quark-antiquark and three quark systems. In the presence of color sources, a characteristic flux-tube structure appears among them, suggesting a linear confining potential. We show that the magnitude of the condensate is reduced inside the color flux, which indicates the partial restoration of chiral symmetry inside the *hadrons*. Considering a periodic box containing a static baryon source, which mimics the *nuclear matter*, we estimate the chiral symmetry restoration in the presence of finite baryon number density.

---

[*]Speaker.

---

1. Introduction

Chiral symmetry is spontaneously broken in the non-perturbative vacuum of QCD. This symmetry breaking is closely related to underlying topological structure of the vacuum, such as the instantons. One of the fundamental order parameters to characterize the vacuum is the chiral condensate $\langle \bar{q}q \rangle$, which has a non-zero expectation value in the vacuum. How it is affected by finite temperature or/and density is an interesting question of the QCD dynamics.

Probing the vacuum with color charges interesting non-trivial structures can be found. For example, a color flux-tube emerges between quark and antiquark, which induces a linearly rising confining potential [1]. This flux-tube can be observed by gluonic degrees of freedom around the color sources from lattice QCD calculations [2, 3]. It is also reported that color charges modify the chiral condensate [3, 4, 5].

In this work, we analyze the chiral condensation near static color sources by using overlap-Dirac eigenfunctions. We discuss the modification of the chiral condensate for both quark-antiquark and three-quark systems made of static quark lines as toy models of hadrons. Considering a single such toy baryon in a periodic box, we can also model the nuclear matter, with which we estimate the size of chiral symmetry restoration at finite density.

2. Partial restoration of chiral symmetry inside hadrons

In this study, we use 2+1-flavor dynamical overlap-fermion configurations, which are generated by the JLQCD Collaboration [6]. The massless overlap-Dirac operator is defined by

$$D_{\text{ov}}(0) = m_0 \left[1 + \gamma_5 \text{sgn} \, H_W(-m_0) \right], \tag{2.1}$$

where $H_W(-m_0) = \gamma_5 D_W(-m_0)$ is the hermitian Wilson-Dirac operator, and sgn denotes the matrix sign function [7, 8]. The overlap-fermion is suited for the study of chiral symmetry and topological properties of QCD [6], as it preserves exact symmetry on the lattice [7]. We use $16^3 \times 48$ and $24^3 \times 48$ lattices at $\beta = 2.3$, which corresponds to a lattice spacing $a^{-1} = 1.759(10)$ GeV. The dynamical quark masses are $m_{\text{ud}} = 0.015a^{-1}$ and $m_{\text{s}} = 0.080a^{-1}$, and the global topological charge is fixed at $Q = 0$.

2.1 Local chiral condensate $\bar{q}q(x)$

In order to study the chiral condensation inside hadrons, we measure the expectation value of the scalar density operator $\bar{q}q(x)$ around static color sources. By using the overlap-Dirac eigenfunction $\psi_\lambda(x)$ and the corresponding eigenvalue λ, which satisfies $D_{\text{ov}}(0)\psi_\lambda = \lambda \psi_\lambda$, the quark-loop due to the insertion of $\bar{q}q(x)$ is written as

$$\bar{q}q(x) = -\sum_\lambda \frac{\psi_\lambda^\dagger(x)\psi_\lambda(x)}{m_q + (1 - \frac{m_q}{2m_0})\lambda}, \tag{2.2}$$

for a quark mass m_q. The chiral condensate $\langle \bar{q}q \rangle$ is given by the spatial average of $\bar{q}q(x)$, which leads to the well-known Banks-Casher relation [9]. Instead of summing over all eigenmodes, we introduce its low-mode approximation by truncating the sum from the lowest eigenvalue to an upper limit, that is set by the number of modes N.

2

We find that the local chiral condensate $\bar{q}q(x)$ forms clusters, which seem to correlate with topological charge distribution (Fig. 1). This result may suggest the instanton-based picture of QCD vacuum [11].
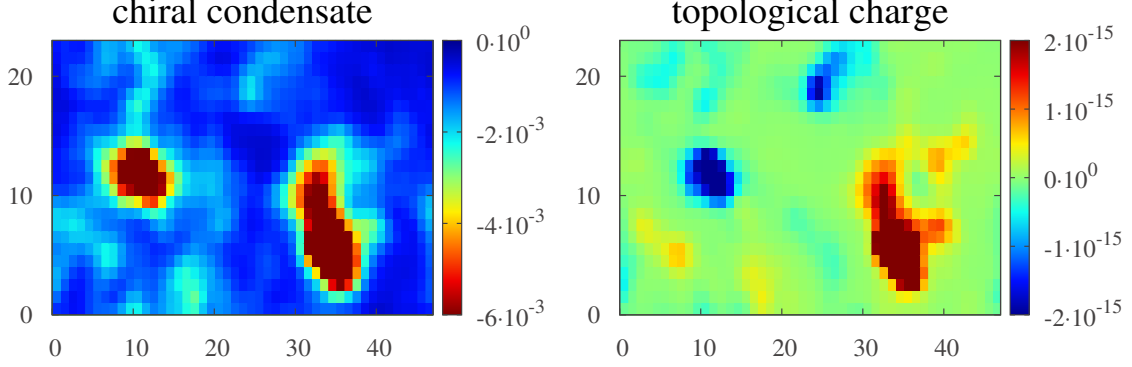

Figure 1: A snapshot of the local chiral condensate and topological charge distribution as calculated using low-lying 20 eigenmodes. The topological charge density is constructed by the Dirac eigenfunction using Gattringer's decomposition [3, 10]. They show an intersection on the same X-T slice of the four-dimensional lattice. Data for 2+1-flavor QCD at $\beta = 2.30$ on a $24^3 \times 48$ lattice.

2.2 Chiral condensate in quark-antiquark system

Now, we discuss the modification of the chiral condensate around the static color sources. We measure a spatial distribution of $\bar{q}q(\vec{x})$ around the static color sources as

$$\langle \bar{q}q(\vec{x}) \rangle_W \equiv \frac{\langle \bar{q}q(\vec{x})W(R,T) \rangle}{\langle W(R,T) \rangle} - \langle \bar{q}q \rangle, \tag{2.3}$$

where $W(R,T)$ is the Wilson loop with the size of $R \times T$, which corresponds to a static quark-antiquark pair with a separation R. A schematic picture of the measurement is shown in Fig. 2 (a).

Figure 2 (b) is the spatial distribution of the local chiral condensate with $R = 10$. The black bars show the positions of the color sources. Here, we use a low-mode truncated condensate $\bar{q}q^{(N)}(\vec{x})$ by truncating the sum at $N = 160$ in Eq. (2.2), which is large enough to discuss the condensate [12]. The valence quark mass is $m_q = 0.015$. In order to improve the signal of the Wilson loop, we adopt the APE smearing for the spatial link-variable, and the temporal extension is set to $T = 4$ where the ground state becomes dominant. The number of configurations is 50.

As shown in Fig. 2 (b), there appears a tube-like structure between color sources, where difference of condensate $\langle \bar{q}q(\vec{x}) \rangle_W$ becomes positive. Since $\langle \bar{q}q \rangle$ is negative in the vacuum, this result implies that the magnitude of chiral condensate is reduced inside the Q$\bar{\text{Q}}$-system.

In order to discuss the restoration quantitatively, the renormalization of the operator $\bar{q}q$ is required. By taking the mode truncation as a regularization scheme [12], the power divergence is parameterized as

$$\langle \bar{q}q \rangle^{(N)} = \langle \bar{q}q^{(\text{subt})} \rangle + c_1^{(N)} m_q/a^2 + c_2^{(N)} m_q^3, \tag{2.4}$$
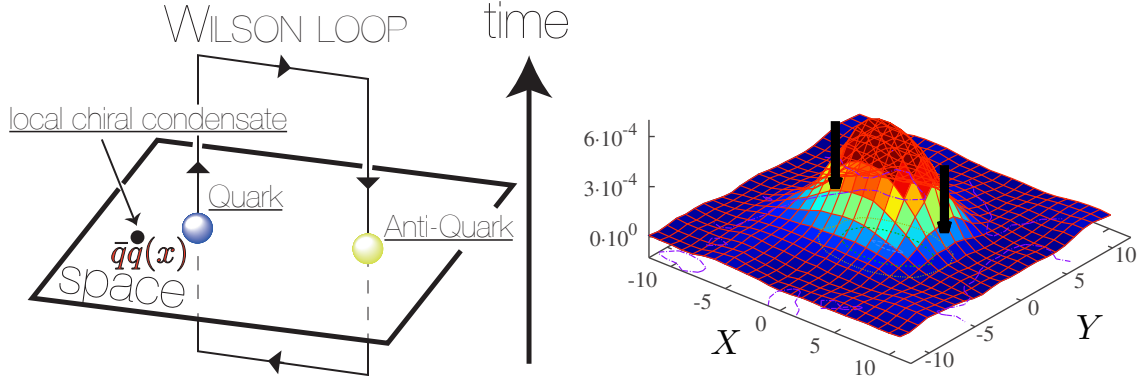
3

Figure 2: (a) A schematic picture of local chiral condensate measurement around quark-antiquark pair. (b) A change of local chiral condensate around quark-antiquark pair. The black bars denote the location of sources at $(X, Y) = (5, 0)$ and $(-5, 0)$.
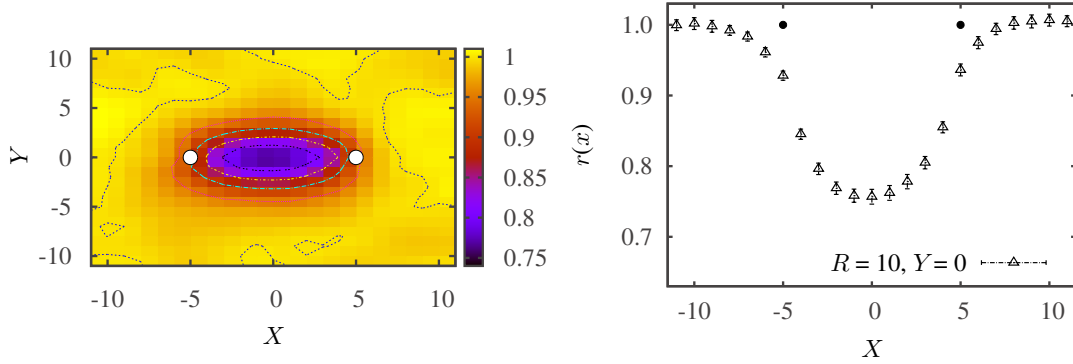

Figure 3: (a) The heat-map of chiral condensate ratio $r(\vec{x})$ around the static color sources, whose locations are depicted by circles. The magnitude of condensate becomes smaller between color sources. (b) The cross-section of $r(\vec{x})$ along static color sources, which are denoted by the black points.

in which the potential $1/a^3$ term is absent because of the exact chiral symmetry of overlap-fermion [7, 8]. These coefficients $c_1^{(N)}$ and $c_2^{(N)}$ may be obtained by fitting $\langle \bar{q}q \rangle^{(N)}$ as a function of m_q. The subtracted condensate $\langle \bar{q}q^{(\text{subt})} \rangle$ becomes finite up to logarithmic renormalization. By taking the ratio,

$$r(\vec{x}) \equiv \frac{\langle \bar{q}q^{(\text{subt})}(\vec{x}) W(R, T) \rangle}{\langle \bar{q}q^{(\text{subt})} \rangle \langle W(R, T) \rangle}, \tag{2.5}$$

the remaining divergence is also canceled.

Figure 3 shows a heat-map of the ratio $r(\vec{x})$ and its cross-section along the flux with $R = 10$. There appears a tube-like region, where magnitude of the chiral condensate is reduced. In particular, the restoration becomes largest around the center of the color charges. In this case, the condensate is reduced by about 25% at the center.

We also show the R dependence of the restoration. Figure 4 (a) is the cross-section of the ratio $r(\vec{x})$ along X-axis with $R = 4$, 8 and 10. The positions of color sources are $X = \pm 2$, ± 4, ± 5, respectively. It is clear that the magnitude of restoration becomes larger with the size of systems.
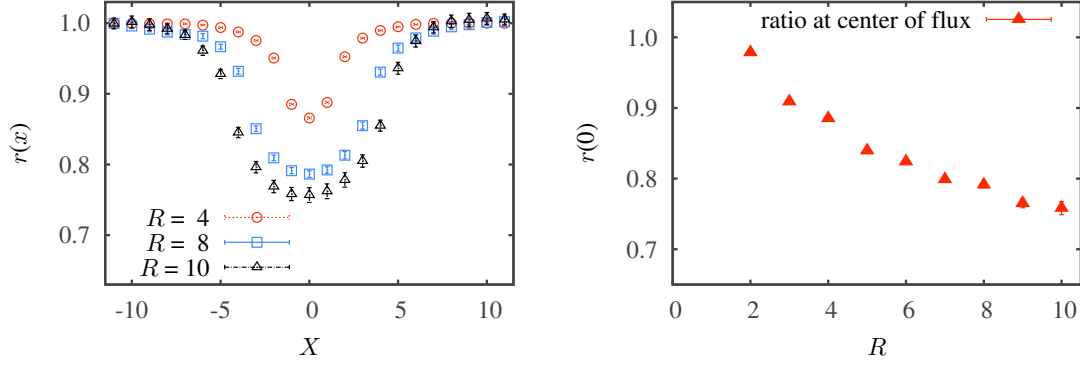
4

Figure 4: (a) The cross-section of chiral condensate ratio with color source separation at $R = 4, 8$, and 10. (b) R-dependence of the ratio at the center of the flux.

Fig. 4 (b) shows the ratio at the center of sources $r(0)$, which decreases monotonically. However, it is unlikely that chiral symmetry is completely restored inside the flux-tube, since a flux-tube is broken through quark-antiquark pair creation. Considering the string breaking scale of around 1 fm [1], the maximum reduction would be at most 30% in the Q$\bar{\text{Q}}$-system.

2.3 Chiral condensate in three quark system

It is also possible to calculate the chiral condensate with multiple color sources. Here, we consider three color sources corresponding to a *baryon*. Using the path-ordered product $U_k \equiv \prod_{\Gamma_k} e^{iagA_k}$ along the path Γ_k, the 3Q-Wilson loop is given by $W_{3Q} \equiv \frac{1}{3}\varepsilon_{abc}\varepsilon_{a'b'c'}U_1^{aa'}U_2^{bb'}U_3^{cc'}$, which is composed to form a color singlet [13]. The ratio of chiral condensate in the 3Q-system $r_{3Q}(\vec{x})$ is given by substituting the 3Q-Wilson loop W_{3Q} for the Wilson loop $W(R,T)$ in Eq. (2.5) [3].

We choose an isosceles right triangle configuration on XY-plane for simplicity. Figure 5 show the chiral condensate ratio $r_{3Q}(\vec{x})$ and its cross-section along $X = Y$ with color sources at $(X,Y) = (0,0)$, $(6,0)$ and $(0,6)$. Similar to the Q$\bar{\text{Q}}$-system, chiral symmetry is partially restored among color sources, where the magnitude of the condensate is reduced. Around the center of sources, the chiral condensate is reduced by about 30%, which is almost the same magnitude as the Q$\bar{\text{Q}}$ case shown in Fig. 3. We note that the characteristic Y-type flux is smeared in Fig. 5, as the thickness of flux is comparable to the separation of color sources [14].

2.4 Partial restoration of chiral symmetry at "finite-density"

Finally, we discuss the partial restoration of chiral symmetry at finite density [15]. Considering a single baryon in the spatial periodic box, it could be regarded as a *nuclear crystal*. In this setup the baryon number density ρ can be defined as $\rho \equiv 1/L^3$ with a spatial lattice size L. Then, the *nuclear matter density* is changed by the spatial volume of the box. We calculate the net change of chiral condensate, which is given by the spatial average of the ratio $r_{3Q}(\vec{x})$ as

$$\frac{\langle\bar{q}q\rangle_\rho}{\langle\bar{q}q\rangle_0} \equiv \frac{1}{L^3}\sum_{\vec{x}}\frac{\langle\bar{q}q(\vec{x})\rangle_{3Q}}{\langle\bar{q}q\rangle} = \frac{1}{L^3}\sum_{\vec{x}}r_{3Q}(\vec{x}). \tag{2.6}$$

We use two lattice volumes $L^3 = 24^3$ and 16^3. These boxes correspond to $\rho \sim 0.3\rho_0$ and $\rho \sim \rho_0$, respectively, with normal nuclear matter density $\rho_0 \simeq 0.18$ fm^{-3}. In this analysis, the size
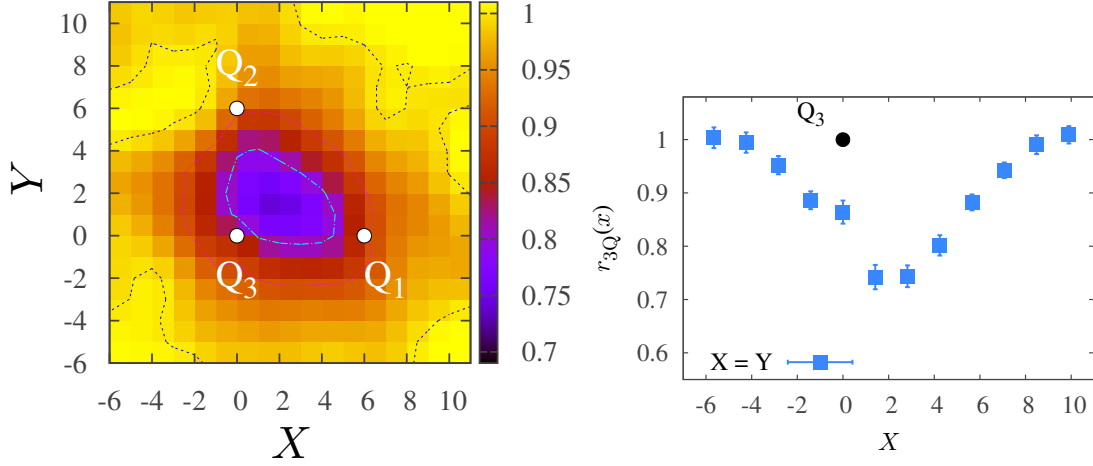
Figure 5: The ratio of chiral condensate around three-static color sources at $(X, Y) = (0,0)$, $(6,0)$ and $(0,6)$. (a) The heat-map of $r_{3Q}(\vec{x})$. (b) The cross-section of $r_{3Q}(\vec{x})$ along $X = Y$.
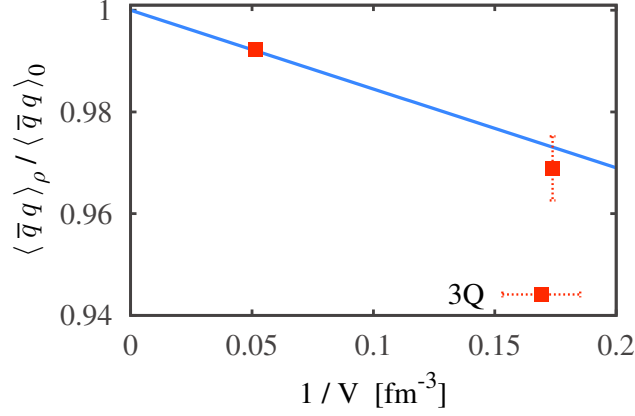

Figure 6: The net change of chiral condensate $\langle \bar{q}q \rangle_\rho / \langle \bar{q}q \rangle$ with the spatial configuration of 3Q color sources at $(X, Y) = (0,0)$, $(6,0)$, and $(0,6)$. We use the two spatial volume 24^3 and 16^3, which corresponds to $\rho \simeq 0.3\rho_0$ and ρ_0, respectively.

of a *baryon* is determined by the shape of the 3Q-Wilson loop. Here, we use the same spatial configuration as in Fig. 5.

Figure 6 shows density dependence of the chiral condensate $\langle \bar{q}q \rangle_\rho / \langle \bar{q}q \rangle_0$, the solid line is a linear fit result from the vacuum expectation value. In the setup shown in Fig. 5, the restoration is estimated to be about 3% at ρ_0. Considering about 30% of the chiral condensate is expected to be reduced in the nuclear matter [15], our result seems small. However, the net change of the condensate in Eq. (2.6) may depend on the size of the baryon. For the setup of Fig. 5, the root mean square radius is about 0.44 fm, which is smaller than that of physical proton or neutron[1]. Similar to the Q$\bar{\text{Q}}$-system shown in Fig. 4, the reduction becomes larger with the size of the 3Q-system. Unfortunately, due to the large statistical errors, it is difficult to numerically calculate larger 3Q-

---

[1]For example, charge root mean square radius of proton is about 0.88 fm.

6

Wilson loop configurations than that in Fig. 5. The reduction of chiral condensate can be more significant at a physical baryon size.

Acknowledgements

References

[1] G. S. Bali, *Phys. Rept.* **343** (2001) 1 [hep-ph/0001312].

[2] G. S. Bali, K. Schilling and C. Schlichter, *Phys. Rev.* **D51** (1995) 5165 [hep-lat/9409005]; P. Cea and L. Cosmai, *Phys. Rev.* **D52** (1995) 5152 [hep-lat/9504008]; R. W. Haymaker, V. Singh, Y. -C. Peng and J. Wosiek, *Phys. Rev.* **D53** (1996) 389 [hep-lat/9406021].

[3] T. Iritani, G. Cossu and S. Hashimoto, PoS (Lattice 2013) 376 [arXiv:1311.0218 [hep-lat]]; PoS (Hadron 2013) 159 [arXiv:1401.4293 [hep-lat]].

[4] M. Faber, M. Schaler, and H. Gausterer, *Phys. Lett. B* **317** (1993) 409; W. Sakuler, W. Burger, M. Faber, H. Markum, M. Muller, P. De Forcrand, A. Nakamura and I. O. Stamatescu, *Phys. Lett. B* **276** (1992) 155; S. Thurner, M. Feurstein, H. Markum, and W. Sakuler, *Phys. Rev.* **D54** (1996) 3457; K. Hübner, PoS (Lattice 2007) 193 [arXiv:0709.1467 [hep-lat]].

[5] H. Suganuma and T. Tatsumi, *Annals Phys.* **208** (1991) 470; *Phys. Lett. B* **269** (1991) 371; *Prog. Theor. Phys.* **90** (1993) 379.

[6] S. Aoki et al. (JLQCD and TWQCD Collaborations), *Prog. Theor. Exp. Phys.* **2012** (2012) 01A106.

[7] P. H. Ginsparg and K. G. Wilson, *Phys. Rev.* **D25** (1982) 2649.

[8] H. Neuberger, *Phys. Lett. B* **417** (1998) 141 [hep-lat/9707022]; *ibid.* **427** (1998) 353 [hep-lat/9801031].

[9] T. Banks and A. Casher, *Nucl. Phys.* **B169** (1980) 103.

[10] C. Gattringer, *Phys. Rev. Lett.* **88** (2002) 221601 [hep-lat/020220].

[11] T. Schäfer and E. V. Shuryak, *Rev. Mod. Phys.* **70** (1998) 323 [hep-ph/9610451].

[12] J. Noaki, T. W. Chiu, H. Fukaya, S. Hashimoto, H. Matsufuru, T. Onogi, E. Shintani and N. Yamada, *Phys. Rev.* **D81** (2010) 034502 [arXiv:0907.2751 [hep-lat]].

[13] T.T. Takahashi, H. Matsufuru, Y. Nemoto, and H. Suganuma, *Phys. Rev. Lett.* **86** (2001) 18; *Phys. Rev.* **D65** (2002) 114509.

[14] H. Ichie, V. Bornyakov, T. Streuer and G. Schierholz, *Nucl. Phys. A* **7121** (2003) 899 [hep-lat/0212036]; *Nucl. Phys. Proc. Suppl.* **119** (2003) 751 [hep-lat/0212024].

[15] R. S. Hayano and T. Hatsuda, *Rev. Mod. Phys.* **82** (2010) 2949 [arXiv:0812.1702 [nucl-ex]].